

1 **STRUCTURAL BUILD-UP OF RIGID FIBER REINFORCED CEMENT-BASED**
2 **MATERIALS**

3

4 A. Perrot^{1*}, T. Lecompte¹, P. Estellé², S. Amziane³

5 (1) Laboratoire d'ingénierie des Matériaux de Bretagne, Université de Bretagne Sud, Université Européenne de
6 Bretagne - Centre de Recherche Christiaan Huygens, BP 92116, 56321 LORIENT Cedex, France

7 (2) Laboratoire de Génie Civil et de Génie Mécanique, Université de Rennes 1, Université Européenne de
8 Bretagne, 3, rue du clos Courtel, BP 90422, 35704 Renne Cedex, France

9 (3) Clermont Université, Université Blaise Pascal, EA 3867, Laboratoire de Mécanique et Ingénieries, BP
10 10448, F-63000 Clermont-Ferrand, France

11

12 *: Corresponding author

13 Arnaud Perrot, Mail: arnaud.perrot@univ-ubs.fr ; Tel: +33 2 97874577; Fax: +33 2 97874576

14

15 **Abstract:**

16 The structural build-up of rigid fiber reinforced cement-based materials is studied. It has
17 recently been shown that the behaviour of fiber reinforced concrete depends on the orientation
18 of the fibers that has to be optimized during casting. As a result, there is a great interest to
19 study the rheology of fiber reinforced concrete. One of the most important characteristic of
20 modern fresh concretes is the structural build-up which is involved in many recent issues of
21 concrete casting. This characteristic depends on the cement pastes chemical activity. This
22 present work shows that structural build-up modelling used for common concretes can be
23 generalized to fiber reinforced concretes. It can be shown that, if the inclusions percolation
24 threshold is not reached, the structural build-up rate A_{thix} is amplified by the addition of fibers
25 and aggregates. Finally, this amplification of the structuration is estimated using modelling
26 initially developed for spherical inclusions and aggregates.

27

28 **1 Introduction**

29

30 Reinforcing concrete with steel fibers improves the mechanical behaviour of the concrete in
31 different ways. It explains why steel fibers reinforced concrete has been the subject of
32 numerous studies in the past recent years (Altun et al. 2007; Ferrara et al. 2007; di Prisco et
33 al. 2009; Rokugo et al. 2009; Tokgoz 2009; Walraven 2009; Wang et al. 2010; Kovler and
34 Roussel 2011). Steel fibers are known to improve the ductility, the tensile behaviour and the
35 resistance to cracking of concrete (Wille et al. 2012; Ferrara et al. 2007; Pujadas et al. 2012;
36 Colombo et al. 2010; Ferrara et al. 2011). It has also been showed that steel fibers increase the
37 flexural strength and hence that steel fibers can be seen as a partial or total alternative to
38 common steel rebars (Katzner and Domski 2012; Michels et al. 2012).

39 Many researchers have pointed out that the efficiency of the steel fibers reinforcement
40 depends on their dispersion and orientation (Boulekbache et al. 2010; Kang and Kim 2011;
41 Boulekbache et al. 2012). As example, tensile and shear strengths are largely influenced by
42 the fibers orientation.

43 Consequently, recent researches have focused on the monitoring of the fibers orientation in
44 order to optimize the aimed mechanical behaviour using two main techniques. The first one
45 consists in using magnetic fields to monitor the fibers orientation (Ferrara et al. 2012a;
46 Ferrara et al. 2012b; Torrents et al. 2012). The second one consists in a flow-induced
47 orientation of the fibers (Boulekbache et al. 2010; Martinie and Roussel 2011; Boulekbache et
48 al. 2012). For the second technique, the material rheological behaviour description is required
49 in order to predict the fibers orientation (Martinie et al. 2010; Martinie and Roussel 2011;
50 Laranjeira et al. 2012; Laranjeira et al. 2011).

51 Rheology of steel fibers reinforced concrete has already been studied by many researchers
52 (Kaufmann et al. 2006; Kuder et al. 2007; Wallevik 2009; Martinie et al. 2010; Martinie and

53 Roussel 2011). Martinie et al. (2010) provides a classification of the fiber stiffness according
54 to the concrete yield stress. They also shows that steel fibers can be considered as rigid if the
55 deformation of the fibers due to shearing remains negligible in front of the fiber length. For
56 such rigid fibers, the authors show that the concrete yield stress depends on a relative packing
57 which depends on the aggregate volume fraction, fiber aspect ratio r (ratio of the fiber length
58 l_f over the fiber diameter d_f) and fiber volume fraction. Such approach provides a simple and
59 efficient tool that can be very helpful for mix-design.

60 However those studies do not focus on the time-dependent behaviour of the concrete (Lapasin
61 et al. 1979; Roussel 2005, 2006; Wallevik 2009). Lapasin et al. have shown that the cement-
62 based pastes are thixotropic (Lapasin et al. 1979). Roussel and co-workers have shown that
63 rheological behaviour of the cement paste at rest exhibits a structural build-up that leads to a
64 linear increase of the yield stress (Roussel 2005, 2006). This behaviour is due to reversible
65 grains nucleation by CSH formation at the grains contact points (Roussel et al. 2012). The
66 structural build-up rate denoted A_{thix} and expressed in $\text{Pa}\cdot\text{min}^{-1}$ is the rate of the yield stress
67 increase of a cement-based material left at rest. It can be easily computed as the slope of the
68 yield stress vs. resting time curve at very early age (few dozens of minutes). This coefficient
69 has been showed to be sufficient to describe casting process issues such as formwork pressure
70 (Ovarlez and Roussel 2006; Tchamba et al. 2008; Perrot et al. 2009) or distinct layer casting
71 (Roussel 2007; Roussel and Cussigh 2008).

72 This study aims to describe the structural build-up behaviour of rigid fiber reinforced cement-
73 based materials. This will help to predict the time of casting and transportation available for
74 fiber reinforced concrete. This present work shows that structural build-up modelling used for
75 common concretes can be generalized to fiber reinforced concretes. Indeed, it is highlighted
76 that the evolution of the yield stress of fiber reinforced concrete at rest is linear and that the
77 structuration rate A_{thix} can be used. For this study, an experimental campaign has been

78 performed. The yield stress of six different mortars has been measured at five different resting
79 times (from 0 to 40 minutes of rest). For each mortar, different fiber volume fractions are
80 added. It can be shown that, if the inclusions percolation threshold is not reached, the
81 structural build-up rate A_{thix} is amplified by the addition of fibers and aggregates. Especially,
82 the influence of relative packing as described by Martinie et al. (Martinie et al. 2010) on the
83 structural build-up coefficient is analysed. A biphasic approach is considered with no
84 physicochemical interactions between the particles and the paste. It is assumed that inclusions
85 do not absorb water, in spite of the fiber high surface exchange. Finally it is shown that the
86 modelling initially developed for spherical inclusions and aggregates (Mahaut et al. 2008b) in
87 order to predict the structural build-up rate are also valid with fibers.

88

89 **2 Materials and methods**

90

91 **2.1 Materials**

92 A CEM I type cement of specific gravity 3.15 is used in this study. Its specific surface
93 measured using a Blaine apparatus is 3390 cm²/g.

94 The sand is a usual Loire river-sand. It has minimum /maximum sizes of 20 μm to 3.15 mm
95 and an absorption capacity of 0.9%.

96 High range water reducing admixture (HRWRA) is also used. It is a polycarboxylate type
97 polymer conditioned in liquid form containing 20 % of dry material. Its recommended dosage
98 ranges from 0.3 to 3% per weight of cement. In this study, two dosages of 1.5% or 2.5% in
99 mass of cement were chosen depending of the studied mortar. The HRWRA is added to the
100 mixing water before water/cement contact.

101 Tested fibers are short steel fibers. Their specific gravity is 7.85 and their young modulus E is
102 210 GPa. They have a length of 6 mm and a diameter of 160 μm leading to an aspect ratio r of
103 37.5.

104 According to the criterion defined by Martinie et al., the ratio of the deflexion f over the fiber
105 length l_f when the fiber is sunk into a cement-based paste exhibiting a yield stress denoted t_0
106 is:

$$107 \quad \frac{f}{l_f} = \frac{\tau_0 r^3}{E} \quad (1)$$

108 For the present fibers, this ratio ranges from 0.012% to 0.12% for a paste yield stress between
109 100 Pa, and 1 kPa. This clearly shows that this type of fiber can be considered as rigid even
110 with firm ordinary concrete (exhibiting a yield stress of the order of 1 kPa).

111 The different mix designs are presented in table 1. Tested fiber volume fraction ranges from 0
112 to 6%, and the sand volume fraction ranges from 0 to 36%. Reference cement pastes, with no
113 aggregate are also tested. Two W/C ratios were tested, with different HRWRA dosage to
114 evaluate the influence of the initial yielding behaviour of the samples on their setting at rest.
115 A total of 29 mixes are tested.

116 Water and HRWRA are mixed with dry powder and fibers in a planetary Hobart mixer. The
117 mixing phase consists in two steps: 2 minutes at 140 rpm and then 3 minutes at 280 rpm.

118

119

120

121

122

123

124

125

N°	Name	W/C	PI/C	S/C	ϕ_f (%)	ϕ_s (%)						
1	CP 1	0.34	0.015	0	0	0						
2					0.05	0						
3					1	0						
4					2	0						
5	CP 1 + 0.14S			0.34	0.015	0.3	0	14				
6							0.5	14				
7							1	14				
8							2	14				
9							5	14				
10							6	14				
11	CP 1 + 0.35S					0.34	0.015	1	0	36		
12									0.5	36		
13									1	36		
14									1.5	35		
15									2	35		
16									3	35		
17	CP 1 + 0.28S	0.34	0.015					0.7	0	28		
18									0.5	28		
19									1	28		
20									1.5	28		
21				2	27							
22				4	27							
23	CP 2			0.29	0.025			0	0	0		
24									1	0		
25									2	0		
26	CP 2 + 0.14S							0.29	0.025	0.3	0	14
27						1	14					
28						2	14					
29						3	14					
30	CP 2 + 0.42S					0.29	0.025			1.2	0	42
31											1	42
32											2	42

126

127 Table 1: Summary of tested mixtures (W/C: water over cement mass ratio, HRWRA/C:

128 HRWRA over cement mass ratio, S/C: sand over cement mass ratio)

129

130 2.2 Structural build-up measurements

131 Different techniques can be used to measure the structural build-up coefficient A_{thix} (Roussel

132 2006; Amziane et al. 2008; Mahaut et al. 2008b; Sleiman et al. 2010; Khayat et al. 2012;

133 Lecompte et al. 2012). Field oriented test methods such as portable vane test, plate test or

134 undisturbed slump flow allow accurate measurements of the structural build up of resting

135 cement-based pastes. In this study, vane test on undisturbed samples is used. This method is
136 accurate and relatively easy to carry out (Mahaut et al. 2008b; Lecompte et al. 2012).

137 An Anton Paar Rheolab QC rheometer equipped with a vane geometry well adapted for
138 cement paste and mortar is used. The vane geometry used in this study consisted of four
139 blades around a cylindrical shaft. The vane height and diameter are respectively 60 mm and
140 40 mm. These dimensions allow for an accurate measurement of the yield stress from 10 to
141 700 Pa. The ratio between fiber length and tool diameter is close to seven and ensures that the
142 measurement provides a value representative of the paste behaviour.

143 Yield stress is the more relevant parameter to study the impact of rheology on common
144 casting process. However its measurement is especially difficult to achieve as the yield stress
145 largely depends on the structuration state of the nucleating cement suspension (Roussel et al.
146 2012). As a result, yield stress of cement based materials increases at rest as the material
147 structurates. Roussel predicts a linear increase of the yield stress τ_0 with resting time (Roussel
148 2005, 2006):

$$149 \quad \tau_0 = \tau_0^i + A_{thix} \cdot t_{rest} \quad (2)$$

150 where t_{rest} is the resting time in minutes, τ_0^i is the yield stress just after mixing, in Pa, and
151 A_{thix} is the structural build up rate, in Pa/minute. As a result, the resting time of the material
152 must always be considered when measuring its yield stress.

153 After mixing, the fiber dispersion and isotropic orientation was checked. Then, the material
154 was slowly poured in five different cylindrical containers of 10 cm in diameter and 15 cm in
155 height. The slow pouring velocity is required in order to avoid the fiber orientation. The
156 containers walls were covered with sandpaper to avoid material slippage during tests. The
157 first vane test is then performed, few seconds after the end of the pouring step and close to
158 one minute after the end of the mixing step. We consider that the first vane test starts the
159 resting period. Also, it can be noted here that a pre-shear phase before each test could not be

160 performed for this specific study as it would have strongly modified the orientation of the
161 fibers in the bowl and the structuration state of the cement paste.

162 A measurement stage was performed during 180 s on the Anton Paar rheometer to obtain the
163 yield stress at five given resting times, following the procedure described by Mahaut et al.
164 (Mahaut et al. 2008b). Stress growth is used to determine the yield stress with an apparent
165 shear rate of 0.001 s^{-1} . At such shear rate, viscosity effects are negligible. As a consequence,
166 the yield stress is computed from the maximum torque value which is required for the onset of
167 the flow, i.e. when the apparent yield stress (static yield stress) is reached on the cylindrical
168 shearing surface:

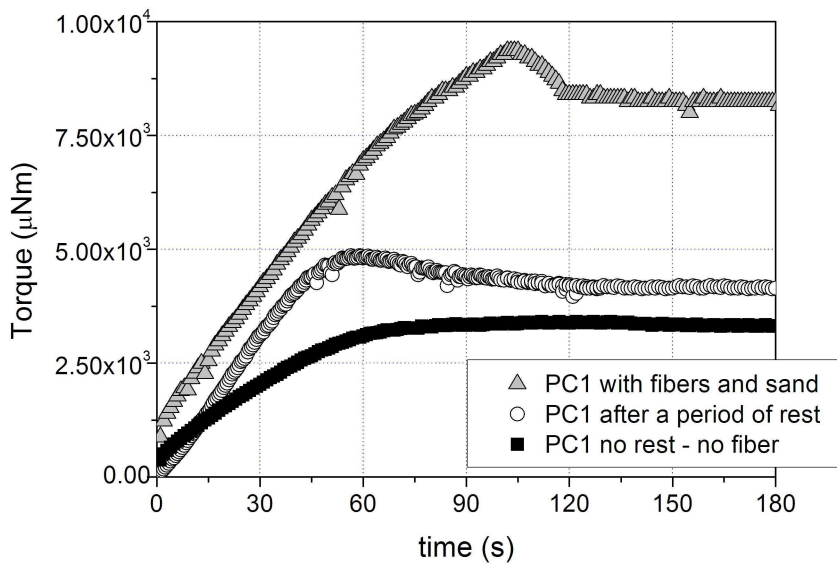
$$169 \quad \tau_0 = \frac{C}{\frac{\pi D^2}{2} \left(H + \frac{D}{3} \right)} \quad (3)$$

170 where C is the torque peak value, H and D are respectively the tool height and diameter.

171 This value depends on the structuration state of the cement-based materials and is different
172 than the dynamic yield stress (intrinsic yield stress) (Roussel 2005). If the material is
173 unstructured (i.e. with no resting time), the torque vs. time curve does not exhibit a peak but a
174 plateau and the dynamic yield stress is measured.

175 Then as shown on figure 1, the torque vs. time curve may present different trends depending
176 on the resting time and the fiber content. With no resting time and no fiber, the curve presents
177 a torque plateau (this is also the case with low amount of fibers). After a resting period or for
178 high fiber content, a peak curve is obtained. This is due to the cement paste destructure
179 after a resting period and to the energy required for the fiber orientation for mix with high
180 amount of fibers (Martinie et al. 2010).

181 Every ten minutes, an undisturbed sample was measured.



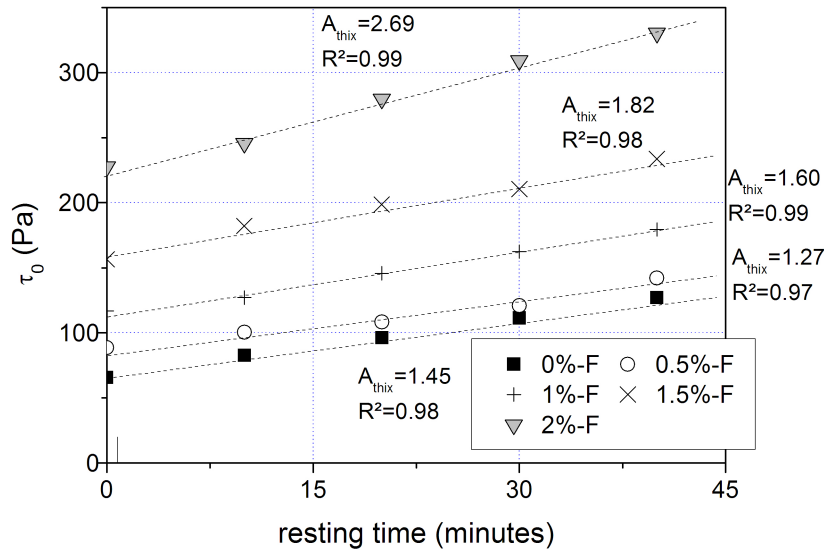
182

183 Figure 1: Typical torque vs. time curves for different scenarios

184

185 3 Results

186 Figure 2 shows the evolution of the yield stress vs. time for the mix CP2-0.28S with different
 187 amount of fibers. It highlights that the Roussel prediction on the linear evolution of yield
 188 stress over resting time accurately describes the material behaviour during the first 40
 189 minutes. It means that the A_{thix} coefficient is sufficient to model the structural build-up
 190 behaviour of the studied materials. The linear increase of yield stress during the first 40
 191 minutes is common to all tested mixes. The measured values of A_{thix} range between 0.37 and 7
 192 $\text{Pa}\cdot\text{min}^{-1}$.



193

194 Figure 2: Yield stress vs. Resting time for different fiber content (CP1-0.28S)

195

196 According to Martinie et al. (2010), the initial yield stress of rigid fiber reinforced concrete
 197 depends on the inclusions relative volume fraction which is defined as the sum of the relative
 198 volume fraction of fibers and the relative volume fraction of the granular skeleton:

$$199 \quad P_f = \phi_f \cdot \frac{r}{4} + \frac{\phi_s}{\phi_m} \quad (4)$$

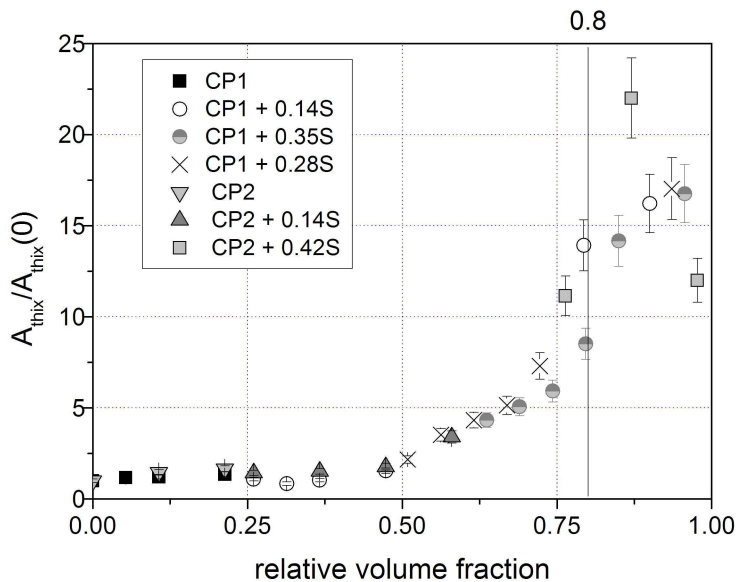
200 where ϕ_s is the volume fraction of sand and ϕ_m is the dense packing fraction of the sand
 201 (Martinie et al. 2010). The ratio $4/r$ represents the dense packing of fibers. According to the
 202 authors, the real global relative volume fraction of the inclusion mixture is probably
 203 underestimated due to wall effects: the decrease of packing fraction of each individual
 204 species close to wall is neglected. Also, we assume that each type of inclusions does not
 205 modify the packing fraction of the other type of inclusion which is probably wrong. For the
 206 used rounded sand, the estimated dense packing fraction is about 0.63.

207 For each mortar, the ratio of its structural build-up rate over the one of the cement paste is
 208 plotted on figure 3, versus the relative volume fraction. All experimental values seem to be on

209 a same curve. It appears that the structural build-up rate follows the same tendency as the
 210 yield stress according to Martinie et al. (Martinie et al. 2010) as it only depends on the
 211 inclusions relative volume fraction. As mentioned by those authors, it is possible to combine
 212 linearly the effects of both fibers and sand in order to identify the rapid increase in the yield
 213 stress of fiber-reinforced cement-based materials around the critical volume fraction at which
 214 all these inclusions combine in order to generate a strong direct contact network in the
 215 material. Below this critical value, the yield stress of the material is close to the suspending
 216 cement paste whereas, above this value, the material yield stress dramatically increases.
 217 Finally, the structural build-up rate of a given mortar can be written as a function of the
 218 relative volume fraction P_f and the cement paste structural build-up A_{thix}^{CP} :

$$219 \quad A_{thix}(\phi_s, \phi_f) = A_{thix}^{CP} \cdot g(P_f) \quad (5)$$

220 Where $g(P_f)$ is a function depending on P_f . This relationship is similar to the one obtained by
 221 Mahaut et al. for mortars (Mahaut et al. 2008b).



222
 223 Figure 3: Non-dimensional structural build-up vs. Relative packing

224 Mahaut et al., based on homogenisation work of Chateau et al. (Chateau et al. 2008; Mahaut
 225 et al. 2008a; Mahaut et al. 2008b), provide an expression to characterise the evolution of the

226 yield stress of a model concrete (with spherical inclusions of the same diameter) as a function
 227 of the yield stress of its cement paste τ_0^{CP} and the volume fraction of it aggregates ϕ_s :

$$228 \quad \tau_0(\phi_s) = \tau_0^{CP} \cdot \sqrt{\frac{1 - \phi_s}{(1 - \phi_s / \phi_{RLP})^{2.5\phi_{RLP}}}} \quad (6)$$

229 Where ϕ_{RLP} is the random loose packing fraction of the aggregates.

230 Combining eq. (2) and (6), it is possible to compute $A_{thix}(\phi_s)$ for any aggregate fraction from
 231 the structural build-up rate of the cement paste A_{thix}^{CP} . As a result, A_{thix} can be written as
 232 follows:

$$233 \quad A_{thix}(\phi_s) = A_{thix}^{CP} \cdot \sqrt{\frac{1 - \phi_s}{(1 - \phi_s / \phi_{RLP})^{2.5\phi_{RLP}}}} \quad (7)$$

234 This has been experimentally verified by Lecompte et al. (Lecompte et al. 2012) on mortars
 235 for aggregate volume fraction ranging from 0 to random loose packing fraction (the range of
 236 application of this modelling).

237 It can be interesting to make an analogy between fibers and aggregates for the prediction of
 238 the structural build-up and yield stress based on the work of Martinie et al. (Martinie et al.
 239 2010). In the work of Mahaut et al., the relative random loose packing fraction writes ϕ_s/ϕ_{RLP} .
 240 According to previous works on granular packing in concrete pastes (Roussel et al. 2010;
 241 Yammine et al. 2008), it is possible to write relative random loose packing fraction versus
 242 dense packing fraction as $\phi_{RLP}=0.8\phi_m$. Then, the relative loose packing fraction for a concrete
 243 or mortar without fibers writes:

$$244 \quad \frac{\phi_s}{\phi_{RLP}} = \frac{\phi_s}{0.8\phi_m} \quad (8)$$

245 Martinie et al. define an equivalent solid volume fraction $\phi_{s,eq}$ for reinforced concretes and
 246 mortars by using equation (4) and multiplying it by the dense packing of sand.

$$247 \quad \phi_{s,eq} = Pf \times \phi_m = \phi_s + \phi_m \cdot \phi_f \cdot r / 4 \quad (9)$$

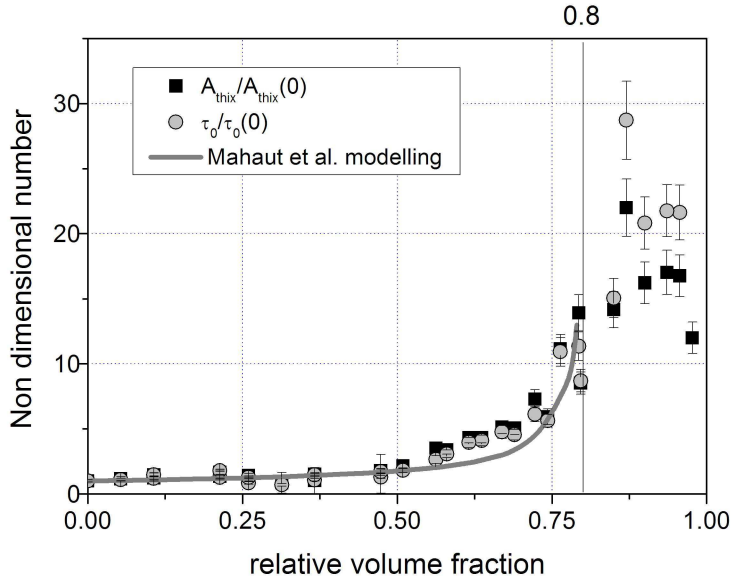
248 Then by analogy, the relative loose packing fraction could become:

$$249 \quad \frac{\phi_{s,eq}}{\phi_{RLP}} = \frac{P_f}{0.8} \quad (10)$$

250 With eq. (9) and (10), it is possible to rewrite the Mahaut et al. relationships (6) and (7) for
251 rigid fiber reinforced cement-based mixes:

$$252 \quad \frac{\tau_0(\phi_s, \phi_f)}{\tau_0^{CP}} = \frac{A_{thix}(\phi_s, \phi_f)}{A_{thix}^{CP}} = \sqrt{\frac{1 - \phi_m P_f}{(1 - P_f / 0.8)^{2.5 P_f / 0.8}}} \quad (11)$$

253 Comparison between experimental relative yield stress, relative structural build-up rate and
254 predictive modelling for rigid fiber reinforced mortar is shown on figure 4. As predicted by
255 Mahaut et al., the relative yield stress and structural build-up rate follow the same evolution in
256 function of the relative volume fraction P_f ranging from 0 to 0.8. One can remark that for $P_f =$
257 0.8, the relative volume fraction is equal to the random loose packing fraction, (see equation
258 10). Then, Mahaut et al. modelling is able to describe the evolution of the studied non-
259 dimensional ratios in the same range of relative volume fraction than for cement-based mixes
260 without fibers. Between $P_f = 0.5$ and $P_f = 0.75$, the modelling slightly underestimates the
261 experimental results, showing the same trend obtained by Lecompte et al. for mortars
262 (Lecompte et al. 2012). An explanation can be that the modelling has been written and
263 validated for monodisperse spheres suspensions. Then, the polydispersity and complex forms
264 of rough sand grains probably induce more energy dissipation that increases the measured
265 shear stress of the tested materials.



266

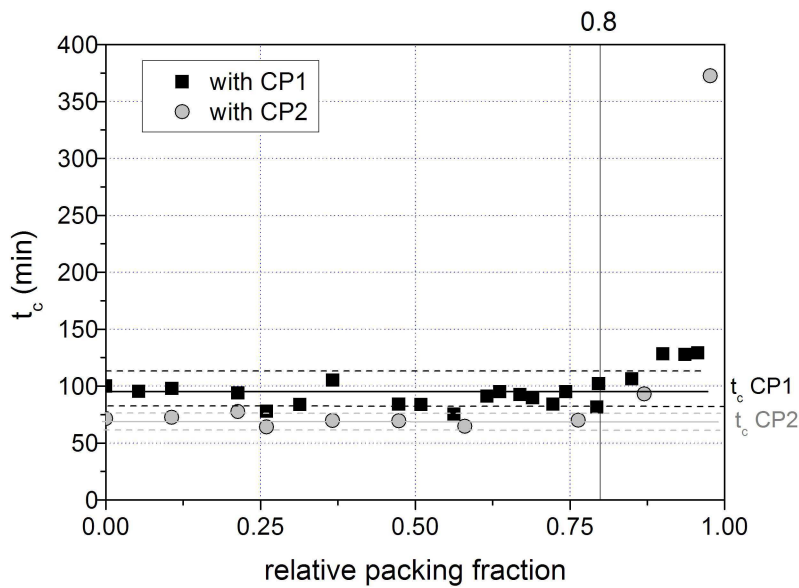
267 Figure 4: Non dimensional structural build-up and yield stress vs. Relative packing.
 268 Comparison with Mahaut et al. predictive modelling (Mahaut et al. 2008a). The plotted
 269 relative yield stresses corresponds to measurements with no resting period (dynamic yield
 270 stress). The non dimensionnel yield stress for the mix CP2-042S with 2% fibers is not plotted
 271 in this figure ($P_f = 0.98$; $\tau_0/\tau_0(0) = 62.3$).

272

273 Another interesting result is the discrepancy between relative yield stress and relative
 274 structural build-up rate observed for relative volume fraction higher than 0.8 where the
 275 relative yield stress presents higher values. This results seems similar to the one obtained by
 276 Lecompte et al. for mortar (Lecompte et al. 2012). The authors show that high content of
 277 inclusions (such as sand and fibers) creates a solid contact network that limits structural build-
 278 up effects.

279 This can be verified by computing a characteristic time t_c which corresponds to the time
 280 required to double the yield stress value ($2 \cdot \tau_0^i = \tau_0^i + A_{thix} \cdot t_c$ leads to $t_c = \tau_0^i / A_{thix}$). Mahaut et
 281 al. write that this ratio does not depend on any solid volume fraction but only on the cement
 282 paste behaviour. This can be easily verified by dividing eq.(6) by eq.(7). Consequently, for all

283 tested mixtures, we should obtain two different values which only depend on the used cement
 284 paste (CP1 or CP2). Figure 5 shows the evolution of the characteristic time t_c versus relative
 285 volume fraction. Average values and standard deviations of t_c are plotted. Those values are
 286 computed separately for each family of mixtures in function of the used cement paste. We
 287 note that average value and standard deviation are computed on mixes with a relative volume
 288 fraction lesser than 0.8.



289
 290 Figure 5: Characteristic structuration time vs. relative packing. Mixes based on cement paste
 291 1 and 2 (CP1 and CP2). Average values (lines) and standard deviations (dot lines) are plotted
 292 in the figure.

293 The figure highlights that the characteristic time t_c does not depend on the relative volume
 294 fraction when $P_f < 0.8$. For higher value of P_f , the characteristic time value is higher than the
 295 one of the cement paste showing that a strong inclusion network slows down structural build-
 296 up effect as shown by Lecompte et al. for mortars (Lecompte et al. 2012).

297
 298
 299

300 **4. Conclusions**

301

302 The evolution of the structural build-up rate of rigid fiber reinforced concrete has been
303 described in function of mix design parameters such as fibers and aggregate volume fraction.
304 Based on the study of Martinie et al. (Martinie et al. 2010) about yield stress of rigid fiber
305 reinforced concrete, it has been shown that the structural build-up rate evolution only depends
306 on the total relative volume fraction, P_f .

307 Then, it has been highlighted that the behaviour of structural build-up depend on the value of
308 P_f :

309 - Beyond 0.8 (i.e. the random loose packing fraction): the relative structural build-up
310 rate (structural build-up rate of the fiber-reinforced mortar over structural build-up rate
311 of its cement paste) follows the same evolution than the relative yield stress described
312 by Martinie et al. (Martinie et al. 2010). In this case, the structural build-up rate can be
313 predicted by an extension of Mahaut et al. modelling adapted to fibers inclusion
314 (Mahaut et al. 2008a; Mahaut et al. 2008b). The characteristic structuration time $t_c(P_f)$
315 which defines the time required to double the initial yield stress of the mix does not
316 depend on the relative volume fraction and is equal to the cement paste characteristic
317 time t_c^{CP} .

318 - Over 0.8, relative yield stress increases faster than the relative structural build-up
319 showing that a strong inclusion network is able to reduce the apparent effect of cement
320 paste structuration.

321

322 **5. References**

323

324 Altun F, Haktanir T, Ari K (2007) Effects of steel fiber addition on mechanical properties of
325 concrete and RC beams. Construction and Building Materials 21 (3):654-661

326 Amziane S, Perrot A, Lecompte T (2008) A novel settling and structural build-up
327 measurement method *Measurement Science and Technology* 19 (10):105702

328 Boulekbache B, Hamrat M, Chemrouk M, Amziane S (2010) Flowability of fibre-reinforced
329 concrete and its effect on the mechanical properties of the material. *Construction and*
330 *Building Materials* 24 (9):1664-1671

331 Boulekbache B, Hamrat M, Chemrouk M, Amziane S (2012) Influence of yield stress and
332 compressive strength on direct shear behaviour of steel fibre-reinforced concrete.
333 *Construction and Building Materials* 27 (1):6-14

334 Chateau X, Ovarlez G, Trung KL (2008) Homogenization approach to the behavior of
335 suspensions of noncolloidal particles in yield stress fluids. *Journal of Rheology* 52
336 (2):489-506

337 Colombo M, di Prisco M, Felicetti R (2010) Mechanical properties of steel fibre reinforced
338 concrete exposed at high temperatures. *Materials and Structures* 43 (4):475-491

339 di Prisco M, Plizzari G, Vandewalle L (2009) Fibre reinforced concrete: new design
340 perspectives. *Materials and Structures* 42 (9):1261-1281

341 Ferrara L, Faifer M, Muhaxheri M, Toscani S (2012a) A magnetic method for non destructive
342 monitoring of fiber dispersion and orientation in steel fiber reinforced cementitious
343 composites. Part 2: Correlation to tensile fracture toughness. *Materials and Structures*
344 45 (4):591-598

345 Ferrara L, Faifer M, Toscani S (2012b) A magnetic method for non destructive monitoring of
346 fiber dispersion and orientation in steel fiber reinforced cementitious composites—
347 part 1: method calibration. *Materials and Structures* 45 (4):575-589

348 Ferrara L, Ozyurt N, Prisco M (2011) High mechanical performance of fibre reinforced
349 cementitious composites: the role of casting-flow induced fibre orientation. *Materials*
350 *and Structures* 44 (1):109-128

351 Ferrara L, Park Y-D, Shah SP (2007) A method for mix-design of fiber-reinforced self-
352 compacting concrete. *Cement and Concrete Research* 37 (6):957-971

353 Kang S-T, Kim J-K (2011) The relation between fiber orientation and tensile behavior in an
354 Ultra High Performance Fiber Reinforced Cementitious Composites (UHPFRCC).
355 *Cement and Concrete Research* 41 (10):1001-1014

356 Katzer J, Domski J (2012) Quality and mechanical properties of engineered steel fibres used
357 as reinforcement for concrete. *Construction and Building Materials* 34 (0):243-248

358 Kaufmann J, Winnefeld F, Hesselbarth D, Trindler W (2006) Evaluation of the consistency of
359 fiber reinforced cementitious composites. *Materials and Structures* 39 (6):645-654

360 Khayat K, Omran A, Naji S, Billberg P, Yahia A (2012) Field-oriented test methods to
361 evaluate structural build-up at rest of flowable mortar and concrete. *Materials and*
362 *Structures*:1-18

363 Kovler K, Roussel N (2011) Properties of fresh and hardened concrete. *Cement and Concrete*
364 *Research* 41 (7):775-792

365 Kuder KG, Ozyurt N, Mu EB, Shah SP (2007) Rheology of fiber-reinforced cementitious
366 materials. *Cement and Concrete Research* 37 (2):191-199

367 Lapasin R, Longo V, Rajgelj S (1979) Thixotropic behaviour of cement pastes. *Cement and*
368 *Concrete Research* 9 (3):309-318

369 Laranjeira F, Aguado A, Molins C, Grünwald S, Walraven J, Cavalaro S (2012) Framework
370 to predict the orientation of fibers in FRC: A novel philosophy. *Cement and Concrete*
371 *Research* 42 (6):752-768

372 Laranjeira F, Grünwald S, Walraven J, Blom C, Molins C, Aguado A (2011)
373 Characterization of the orientation profile of steel fiber reinforced concrete. *Materials*
374 *and Structures* 44 (6):1093-1111

375 Lecompte T, Perrot A, Picandet V, Bellegou H, Amziane S (2012) Cement-based mixes:
 376 Shearing properties and pore pressure. *Cement and Concrete Research* 42 (1):139-147
 377 Mahaut F, Chateau X, Coussot P, Ovarlez G (2008a) Yield stress and elastic modulus of
 378 suspensions of noncolloidal particles in yield stress fluids. *Journal of Rheology* 52
 379 (1):287-313
 380 Mahaut F, Mokeddem S, Chateau X, Roussel N, Ovarlez G (2008b) Effect of coarse particle
 381 volume fraction on the yield stress and thixotropy of cementitious materials. *Cement*
 382 *and Concrete Research* 38 (11):1276-1285
 383 Martinie L, Rossi P, Roussel N (2010) Rheology of fiber reinforced cementitious materials:
 384 classification and prediction. *Cement and Concrete Research* 40 (2):226-234
 385 Martinie L, Roussel N (2011) Simple tools for fiber orientation prediction in industrial
 386 practice. *Cement and Concrete Research* 41 (10):993-1000
 387 Michels J, Waldmann DI, Maas S, Zürbes A (2012) Steel fibers as only reinforcement for flat
 388 slab construction: Experimental investigation and design. *Construction and Building*
 389 *Materials* 26 (1):145-155
 390 Ovarlez G, Roussel N (2006) A Physical Model for the Prediction of Lateral Stress Exerted
 391 by Self-Compacting Concrete on Formwork. *Materials and Structures* 39 (2):269-279
 392 Perrot A, Amziane S, Ovarlez G, Roussel N (2009) SCC formwork pressure: Influence of
 393 steel rebars. *Cement and Concrete Research* 39 (6):524-528
 394 Pujadas P, Blanco A, de la Fuente A, Aguado A (2012) Cracking behavior of FRC slabs with
 395 traditional reinforcement. *Materials and Structures* 45 (5):707-725
 396 Rokugo K, Kanda T, Yokota H, Sakata N (2009) Applications and recommendations of high
 397 performance fiber reinforced cement composites with multiple fine cracking
 398 (HPFRCC) in Japan. *Materials and Structures* 42 (9):1197-1208
 399 Roussel N (2005) Steady and transient flow behaviour of fresh cement pastes. *Cement and*
 400 *Concrete Research* 35 (9):1656-1664
 401 Roussel N (2006) A thixotropy model for fresh fluid concretes: Theory, validation and
 402 applications. *Cement and Concrete Research* 36 (10):1797-1806
 403 Roussel N (2007) Rheology of fresh concrete: from measurements to predictions of casting
 404 processes. *Materials and Structures* 40 (10):1001-1012
 405 Roussel N, Cussigh F (2008) Distinct-layer casting of SCC: The mechanical consequences of
 406 thixotropy. *Cement and Concrete Research* 38 (5):624-632
 407 Roussel N, Lemaître A, Flatt RJ, Coussot P (2010) Steady state flow of cement suspensions:
 408 A micromechanical state of the art. *Cement and Concrete Research* 40 (1):77-84
 409 Roussel N, Ovarlez G, Garrault S, Brumaud C (2012) The origins of thixotropy of fresh
 410 cement pastes. *Cement and Concrete Research* 42 (1):148-157
 411 Sleiman H, Perrot A, Amziane S (2010) A new look at the measurement of cementitious paste
 412 setting by Vicat test. *Cement and Concrete Research* 40 (5):681-686
 413 Tchamba JC, Amziane S, Ovarlez G, Roussel N (2008) Lateral stress exerted by fresh cement
 414 paste on formwork: Laboratory experiments. *Cement and Concrete Research* 38
 415 (4):459-466
 416 Tokgoz S (2009) Effects of steel fiber addition on the behaviour of biaxially loaded high
 417 strength concrete columns. *Materials and Structures* 42 (8):1125-1138
 418 Torrents J, Blanco A, Pujadas P, Aguado A, Juan-García P, Sánchez-Moragues M (2012)
 419 Inductive method for assessing the amount and orientation of steel fibers in concrete.
 420 *Materials and Structures*:1-16
 421 Wallevik JE (2009) Rheological properties of cement paste: Thixotropic behavior and
 422 structural breakdown. *Cement and Concrete Research* 39 (1):14-29
 423 Walraven J (2009) High performance fiber reinforced concrete: progress in knowledge and
 424 design codes. *Materials and Structures* 42 (9):1247-1260

- 425 Wang X, Jacobsen S, Lee S, He J, Zhang Z (2010) Effect of silica fume, steel fiber and ITZ
426 on the strength and fracture behavior of mortar. *Materials and Structures* 43 (1):125-
427 139
- 428 Wille K, Naaman A, El-Tawil S, Parra-Montesinos G (2012) Ultra-high performance concrete
429 and fiber reinforced concrete: achieving strength and ductility without heat curing.
430 *Materials and Structures* 45 (3):309-324
- 431 Yamine J, Chaouche M, Guerinet M, Moranville M, Roussel N (2008) From ordinary
432 rheology concrete to self compacting concrete: A transition between frictional and
433 hydrodynamic interactions. *Cement and Concrete Research* 38 (7):890-896
434
435